Pan American Congress of Applied Mechanics (PACAM-III),
Sao Paulo, Brazil, Jan. 4-8, 1993

ELECTROHYDRODYNAMIC FLOW SIMULATION

George S. Dulikravich
Associate Professor
Department of Aerospace Engineering, 233 Hammond Building
The Pennsylvania State University, University Park, PA 16802, USA

ABSTRACT

A mathematical model and an explicit iterative algorithm for three-dimensional laminar steady flow of an incompressible viscous neutrally charged carrier fluid injected with an electrically charged fluid and exposed to an electric field were developed. Thermally induced buoyancy was incorporated via an extended Boussinesque approximation while including Joule heating effect. due to induced current. Numerical results demonstrate bending of a stream of charged particles under the influence of the steady electric field and an electrohydrodynamic flow instability.

ANALYTICAL AND NUMERICAL MODEL

Electrohydrodynamics (EHD) and Magnetohydrodynamics (MHD) represent two extreme models for a general fluid flow under the influence of electromagnetic fields [1-3]. The EHD model [3] assumes that there is no magnetic field applied or induced, while the MHD model [2] assumes that there are no charged particles in the flow field and that there is no electric potential applied. In EHD flows, a steady electric field is applied to a fluid containing electrically differently charged particles which deflect differently under the influence of the electric field thus separating from each other. Applications of EHD are very diverse and involve ink-jet printers, electrostatic precipitators, electroplating, and various casting and electrophoretic separation devices [3-5].

The mathematical model presented in this paper consists of a neutral carrier fluid with a single specie of charged fluid [3]. This model can be extended to multi-specie problems including a non-neutral carrier fluid. The system of governing equations is derived from a combination of Maxwell's equations of electrodynamics and the Navier-Stokes equations. An idealized charged fluid is assumed and therefore magnetic fields can be neglected. Maxwell's equations reduce to the charge conservation equation and the equation for electric potential. For computational purposes the system of equations can be written in conservative vector form in ξ,η,ζ curvilinear coordinates

$$\frac{\partial \tilde{Q}}{\partial t}+\frac{\partial \tilde{E}}{\partial \xi}+\frac{\partial \tilde{F}}{\partial \eta}+\frac{\partial \tilde{G}}{\partial \zeta}=D^{2}(J\tilde{Q})+\tilde{H} \tag{1}$$

To make this system of equations hyperbolic in time, an artificial compressibility concept was applied [6] by adding a p/β term to the mass conservation equation. The non-dimensional solution vector, $\tilde{Q}$, flux vectors $\tilde{E}$, $\tilde{F}$, $\tilde{G}$ and source vector $\tilde{H}$ expressed in ξ,η,ζ coordinates are:

$$\tilde{Q}=\frac{1}{J}\begin{bmatrix} p/\beta \\ u \\ v \\ w \\ \theta \\ q \end{bmatrix} \quad \tilde{E}=\frac{1}{J}\begin{bmatrix} U \\ Uu+\xi_x p \\ Uv+\xi_y p \\ Uw+\xi_z p \\ U\theta \\ q(U+\frac{1}{RePr_E}E_\xi) \end{bmatrix} \quad \tilde{F}=\frac{1}{J}\begin{bmatrix} V \\ Vu+\eta_x p \\ Vv+\eta_y p \\ Vw+\eta_z p \\ V\theta \\ q(V+\frac{1}{RePr_E}E_\eta) \end{bmatrix} \quad \tilde{G}=\frac{1}{J}\begin{bmatrix} W \\ Wu+\zeta_x p \\ Wv+\zeta_y p \\ Ww+\zeta_z p \\ W\theta \\ q(W+\frac{1}{RePr_E}E_\zeta) \end{bmatrix} \tag{2}$$

With the electric field $\boldsymbol{E}$ defined as $\boldsymbol{E}=(E_\xi,E_\eta,E_\zeta)$ or as $\boldsymbol{E} = -\nabla\Phi$, the source vector becomes

$$\tilde{H}=\frac{1}{J}\begin{bmatrix} 0 \\ \frac{Gr}{Re}n_\xi+S_E q E_\xi \\ \frac{Gr}{Re}n_\eta+S_E q E_\eta \\ \frac{Gr}{Re}n_\zeta+S_E q E_\zeta \\ S_E Ec\left[q\left(v+\frac{1}{RePr_E}E\right)-\frac{1}{ReD_E}\nabla q\right]\cdot E \\ 0 \end{bmatrix} \qquad (3)$$

Here, the viscous terms are defined as $D^2(J\tilde{Q}) = \left[\frac{S}{J}g_{ij}\left(J\tilde{Q}\right)_{,j}\right]_{,i}$, while $\nabla^2\Phi = -N_E q$. (4)

The Jacobian determinant of the geometric transformation from physical into computational space is $J=\frac{\partial(\xi,\eta,\zeta)}{\partial(x,y,z)}$, g_{ij} is the contravariant metric tensor, $\tilde{v}=(u,v,w)^T$ denotes the velocity field with U,V,W as its contravariant components, p is the pressure, q is the electric charge density, θ is the nondimensional temperature, Φ is the electric potential, and S is the diagonal matrix 1/Re diag(0,1,1,1/Pr,1/D_E). Non-dimensional numbers: Reynolds number Re, Prandtl number Pr, Eckert number Ec, Grashof number Gr are defined in a standard way while the charge diffusivity characteristic (D_E), the Lorentz force characteristic (S_E), the electric field characteristic (N_E) and the electric Prandtl number (Pr_E) are defined as:

$$D_E=\frac{\mu}{\rho D} \qquad S_E=\frac{q_r\Phi_r}{\rho v_r^2} \qquad N_E=\frac{q_r L^2}{\varepsilon\Phi_r} \qquad Pr_E=\frac{\mu}{\rho b\Phi_r} \qquad (5)$$

Here, ρ, L, μ, c_p, ε represent fluid density, characteristic length, dynamic viscosity, specific heat, electric permitivity, while subscript r denotes reference values. The diffusivity coefficient, D, and mobility coefficient, b, are related by Einstein's relation [5,3]. The electric permitivity ε was assumed to be uniform and constant. The system of equations given by (1) was solved using a four-stage Runge-Kutta explicit time stepping method [7]. Second and fourth order artificial dissipation were added to improve the numerical stability of the iterative algorithm.

RESULTS

The first test case corresponds to free flow electrophoretic separation in microgravity where temperature is constant along the chamber boundaries and Joule heating and buoyancy force effects are negligible. The charged fluid was injected at the centerline of an electrically neutral aqueous carrier fluid flow. A steady electric field of 7000 V/m was imposed along the side walls. The non-dimensional numbers for this flow were: Re=6.67, Pr=7.9, S_E=0.15, N_E=0.204, Pr_E= 2.8. A non-clustered computational grid consisting of 60 × 30 grid cells was used. As a consequence of the imposed steady electric field, the charged fluid is deflected from the centerline (Fig. 1) as it is carried by the carrier fluid along the chamber. To improve the convergence rate of the iterative process and to smooth out spatial oscillations (Fig. 2) of the concentration of the charged particles, a small amount of second and fourth order artificial dissipation was added. It was observed that even a very small amount of artificial dissipation has a detrimental effect on the accuracy of the predicted diffusion of the charged particles (Fig. 3). Better results were obtained (Fig. 4) by forcing charge density to be non-negative during the iterations, but then convergence rate decreased

The second test case represents an example of a flow instability induced by the electric field where electroconvective vortices analogous to thermoconvective vortices in Benard cells will be developed if sufficient electrical potential energy can be released by inverting a charged fluid layer. In a closed container of aspect ratio AR=3 the charges were initially equally distributed along the lower wall. An external steady electric field was imposed by means of electrodes along the lower and the upper walls. In this case, Joule heating and buoyancy force were taken into account. Nondimensional numbers were Re=1, Pr=1, Gr=3000, Ec=1, S_E=1, N_E=1000, Pr_E=1. Temperature was kept constant along the boundaries. Four well defined vortices induced by the electric field (Fig. 5) have developed causing pressure non-uniformities (Fig.6).

The third test case involved a closed container with the aspect ratio AR=6, having electric potential difference between two vertical walls of 7000 V/m, temperature difference between top (cold) and bottom (warm) wall of 2 K, and gravity acting downwards. Strong electroconvective and thermal buoyancy driven recirculation pattern (Figs. 7-8) developed in this case.

SUMMARY

The mathematical model, the numerical algorithm and the computer code were able to demonstrate the basic principles and phenomenas of the free flow electrophoretic separation where particles having different electric charges are deflected differently under the imposed electric field.

REFERENCES

[1] Stuetzer, O. M., "Magnetohydrodynamics and Electro hydrodynamics", *The Physics of Fluids,* Vol. 5, No. 5, pp. 534-544, (May 1962).

[2] Lee, S. and Dulikravich, G. S., "Magnetohydrodynamic Steady Flow Computations in Three Dimensions", AIAA Paper 91-0388, Reno, NV, (Jan. 1991); also in *Int. Journal of Numerical Methods in Fluids,* Vol. 13, No. 7, pp. 917-936, (Oct. 1991).

[3] Lee, S., Dulikravich, G.S. and Kosovic, B.,"Electrohydrodynamic (EHD) Flow Modelling and Computations", AIAA Paper 91-1469, AIAA Fluid, Plasma Dynamics and Lasers Conference, Honolulu, Hawaii, June 24-26, 1991c.

[4] Melcher, J. R., Continuum Electromechanics, The MIT Press, Cambridge, (1981).

[5] Babskii, V. G., Zhukov, M. Y. and Yudovich, V. I., "Mathematical Theory of Electrophoresis," (translated by C. Flick), Consultants Bureau, New York, (1989).

[6] Chorin, A. J., "A Numerical Method for Solving Incompressible Viscous Flow Problems", *Journal of Computational Physics*, Vol. 2, pp. 12-26.,(1967).

[7] Jameson, A., Schmidt, W., and Turkel, E., "Numerical Solutions of the Euler Equations by Finite Volume Methods Using Runge-Kutta Time-Stepping Scheme," AIAA paper 81-1259, Palo Alto, CA, (June 1981).

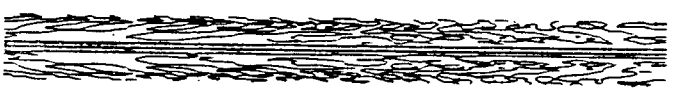

Fig. 1 Charge density pattern in a straight channel flow.

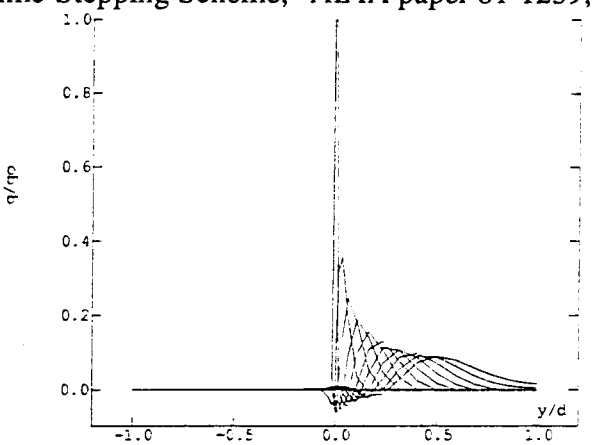

Fig. 2 Charge density profiles at different stations in a channel: no dissipation.

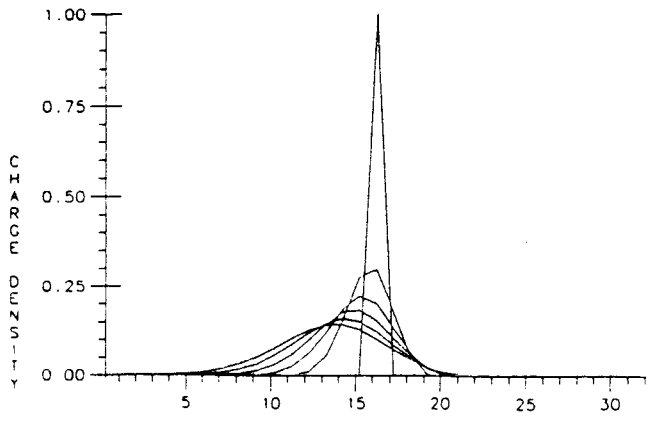

Fig. 3 Charge density profiles at different stations in a channel: large dissipation.

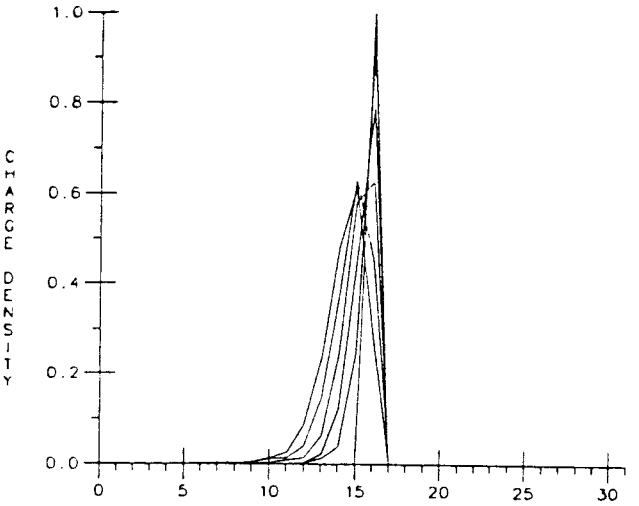

Fig. 4 Charge density profiles at different stations in a channel: small dissipation

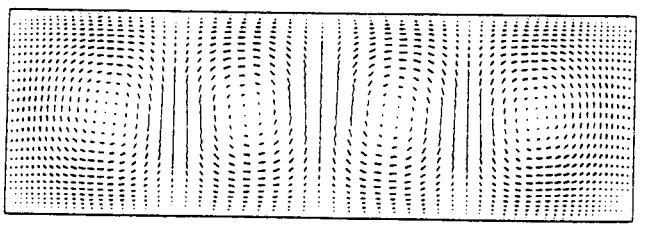

Fig. 5 Electro-thermo-convective vortices in AR=3 container: velocity vector pattern.

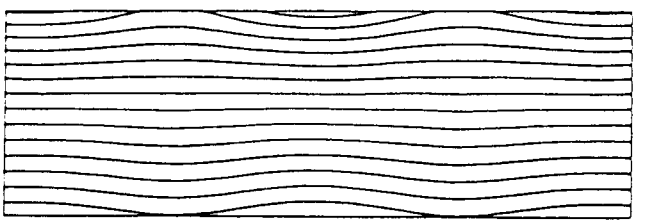

Fig. 6 Electro-thermo-convective vortices in AR=3 container: pressure field.

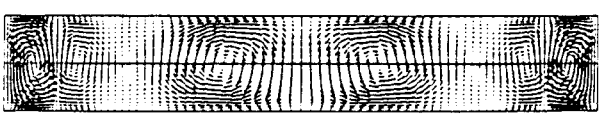

Fig. 7 Electro-thermo-convective vortices in AR=6 container: velocity vector pattern.

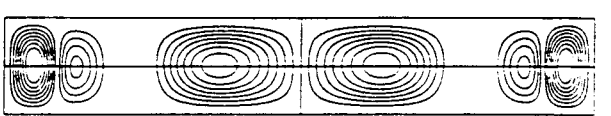

Fig. 8 Electro-thermo-convective vortices in AR=6 container: streamlines.